



**HAL**  
open science

## Blocking bacterial entry at the adhesion step reveals dynamic recruitment of membrane and cytosolic probes

Yann Ciczora, Sébastien Janel, Magali Soyer, Michka Popoff, Elisabeth Werkmeister, Frank Lafont

### ► To cite this version:

Yann Ciczora, Sébastien Janel, Magali Soyer, Michka Popoff, Elisabeth Werkmeister, et al.. Blocking bacterial entry at the adhesion step reveals dynamic recruitment of membrane and cytosolic probes. *Biology of the Cell*, 2019, 111 (3), pp.67-77. 10.1111/boc.201800070 . hal-02347524

**HAL Id: hal-02347524**

**<https://hal.science/hal-02347524>**

Submitted on 24 May 2022





**HAL** is a multi-disciplinary open access archive for the deposit and dissemination of scientific research documents, whether they are published or not. The documents may come from teaching and research institutions in France or abroad, or from public or private research centers.

L'archive ouverte pluridisciplinaire **HAL**, est destinée au dépôt et à la diffusion de documents scientifiques de niveau recherche, publiés ou non, émanant des établissements d'enseignement et de recherche français ou étrangers, des laboratoires publics ou privés.



Distributed under a Creative Commons Attribution - NonCommercial 4.0 International License

# Blocking bacterial entry at the adhesion step reveals dynamic recruitment of membrane and cytosolic probes

Yann Ciczora\*, Sébastien Janel\* , Magali Soyer\*, Michka Popoff\*† , Elisabeth Werkmeister\*   
and Frank Lafont\*<sup>1</sup> 

\*Cellular Microbiology and Physics of Infection Group, Center for Infection and Immunity of Lille, CNRS UMR8204, INSERM U1019, Institut Pasteur de Lille, Lille regional Univ. Hosp. Centr., Lille Univ., Lille F-59019, France and †Institut d'Electronique, de Microélectronique et de Nanotechnologie, CNRS UMR8520, Avenue Poincaré, Villeneuve d'Ascq F-59625, France

**Background.** Bacterial invasion covers two steps: adhesion and entry *per se*. The cell signalling response is triggered upon pathogen interaction at the cell surface. This response continues when the pathogen is internalised. It is likely that these two steps activate different molecular machineries. So far, it has not been possible to easily follow in physiological conditions these events separately. We thus developed an approach to uncouple adhesion from entry using atomic force microscopy (AFM)-driven force and fluorescence measurements.

**Results.** We report nanometric-scale, high-resolution, functional dynamic measurements of bacterial interaction with the host cell surface using photonic and adhesion force analyses. We describe how to achieve a precise monitoring of iterative cell–bacterium interactions to analyse host cell signalling responses to infection. By applying this method to *Yersinia pseudotuberculosis*, we first unveil glycosylphosphatidylinositol-anchored protein domains recruitment to the bacterium cell surface binding site and concomitant cytoskeleton rearrangements using super-resolution fluorescence microscopy. Second, we demonstrate the feasibility of monitoring post-translationally modified proteins, for example, via ubiquitylation, during the first step of infection.

**Conclusion.** We provide an approach to discriminate between cellular signalling response activated at the plasma membrane during host–pathogen interaction and that is triggered during the internalisation of the pathogen within the cell.

**Significance.** This approach adds to the technological arsenal to better understand and fight against pathogens and beyond the scope of microbiology to address conceptual issues of cell surface signalling.



Additional supporting information may be found online in the Supporting Information section at the end of the article.

<sup>1</sup>To whom correspondence should be addressed (email: frank.lafont@pasteur-lille.fr)

**Key words:** Adhesion force, AFM, Correlative microscopy, Super-resolution microscopy, ubiquitin.

**Abbreviations:** AFM, atomic force microscope; CLAM, correlative light AFM microscopy; GFP, green fluorescent protein; GPI, glycosylphosphatidylinositol; MEM, minimum essential media; PALM, photoactivated localisation microscopy; PRR, pattern recognition receptors; STORM, stochastic optical reconstruction microscopy; TIRF, total internal reflection fluorescence; TRAF6, TNF receptor-associated factor 6; YFP, yellow fluorescent protein.

## Introduction

As antibiotic treatment efficiency is limited by the occurrence of multi-resistant strains, it is important to better understand the early stages of infection in order to develop drug discovery strategies targeting host–pathogen interactions. Immediate early

This is an open access article under the terms of the Creative Commons Attribution-NonCommercial License, which permits use, distribution and reproduction in any medium, provided the original work is properly cited and is not used for commercial purposes.

detection of pathogen infection requires the host to sense adhesion of the bacterium to the cell surface. This adhesion step is mediated by ligand–receptor interactions and/or the injection of bacterial effectors through bacterial secretion systems [Dewoody *et al.*, 2013; Mikula *et al.*, 2013]. These interactions modulate cytoskeleton organisation to favour strong interaction of extracellular bacteria with the host cell surface as for the formation of pedestal-like extrusions in the case of enteropathogenic *Escherichia coli* [Cantey *et al.*, 1981] or membrane protrusion for *Neisseria meningitidis* [Hoffmann *et al.*, 2001]. Alternatively, these interactions facilitate invasion with formation of membrane ruffles for the ‘trigger’ mechanism of bacterial entry or plasma membrane invagination for the ‘zipper’ mechanism [Cossart and Sansonetti, 2004]. Also occurring at this initial stage of infection, the cellular innate immune response is triggered quickly upon interaction [Kawai and Akira, 2010]. This response is activated by the engagement of the pattern recognition receptors (PRR) consecutive to their recognition of pathogen–associated molecular patterns [Kawai and Akira, 2011] synthesised by the pathogen. Upon interaction with the pathogen surface PRRs (*e.g.*, Toll-like and C-type lectin receptors) are activated. Cytoplasmic PRRs are triggered by intracytoplasmic replicating bacteria. For example, strong evidence suggests that *Shigella* activates the cytoplasmic PRR nucleotide oligomerisation domain (NOD) proteins to trigger a signalling cascade that induces autophagy mechanisms [Suzuki *et al.*, 2007; Dupont *et al.*, 2009, 2010; Travassos *et al.*, 2010]. On the other hand, before reaching the cytoplasm, listeria hijacks the MET surface receptor that has a large spectrum of downstream effects including the activation of innate immune response [Cossart and Sansonetti, 2004; McCall-Culbreath *et al.*, 2008]. In that instance, the cell develops a complex sensing response that involves many aspects of cell mechanics [Mostowy *et al.*, 2011]. Hence, it is remarkable that upon adhesion, bacteria trigger a variety of events with different time frames. An important control and modulation of the signalling response at the adhesion step operates through strongly regulated post-translational modifications of proteins recruited to the entry site [Ribet and Cossart, 2010b].

A crucial point in order to decipher the sequential molecular orchestration of the host cell response is to consider that these cellular receptors and

signalling machineries continue to be activated during the entry process of invading pathogens. Indeed, after entry, bacteria are internalised within a membrane compartment on which signalling complexes are still present. These complexes undergo further modifications, which coordinate downstream immune/inflammatory responses and membrane trafficking pathways. Distinguishing between adhesion- and internalisation-mediated signalling is technically challenging but would open up new opportunities in drug discovery. Precluding adhesion leads to a complete shutdown of the signalling response, whereas targeting bacteria once internalised inside the cell does not impair signalling pathways triggered upon adhesion.

Since bacterial entry is a fast process, our aim was to block it at the adhesion step long enough to be able to analyse recruitment of different classes of molecules (*i.e.*, membrane and cytosolic proteins). We therefore designed a means of blocking internalisation whilst maintaining adherence between the cell surface and the enterobacterium *Yersinia pseudotuberculosis* (the ancestor of the plague agent *Yersinia pesti*) [Achtman *et al.*, 1999]. *Y. pseudotuberculosis* is a transient enteroinvasive pathogen that breaches the intestinal epithelium, but multiply mostly extracellularly at the *lamina propriae*. *Y. pseudotuberculosis* causes illnesses that range from chronic diarrhoea and mesenteric adenitis to fatal episodes of septicemia in disseminated cases, and is associated to East scarlet-like (Izumi) fever and skin complaints (*erythema nodosum*, reactive arthritis). Internalisation, innate immune modulation and host cell fate depends on both bacterial adhesion proteins and secretion system effectors [Mikula *et al.*, 2013; Chung and Bliska, 2015].

A part from imaging studies of cell surfaces, atomic force microscopy (AFM) was used to analyse (i) the effect of drug treatment on bacteria physics properties, (ii) the interactions of bacteria:substratum and bacteria:single molecule from the substratum, bacteria or the host [Alsteens *et al.*, 2013; Xiao and Duf re, 2016]. Moreover, bacteria-functionalised cantilevers are used to probe bacteria:host cell interactions [*e.g.*, Feuillie *et al.*, 2018; Prystopiuk *et al.*, 2018]. However, herein we propose to analyse on line the adhesion of bacteria on the host cell while following in high resolution fluorescent microscopy the recruitment of proteins from the host. Coupling of AFM to super-resolution has already been pioneered by the

Diaspro's Group and since documented by several groups including ours [Harke *et al.*, 2012; Janel *et al.*, 2017]. Here, we performed experiments while maintaining the bacterium at the cell surface in order to follow the recruitment of host cell proteins at the adhesion step. This successfully reveals the potential for online recording, at high resolution, the immediate cell signalling response subsequent to this first step in the entry process. Because it is extendable to cell-cell interactions, it also interests other physiological disorders and fields as cell biology and cell physics.

## Results

### GPI dynamics upon bacteria landing on the host cell

In our set-up model, we immobilised a single bacterium on a tipless cantilever of an atomic force microscope. We then used the cantilever to land the bacterium onto the cell surface. Thus, we monitored, thanks to several correlative light AFM microscopy (CLAM) setups [involving video microscopy, video-total internal reflection fluorescence (TIRF) microscopy, photoactivated localisation microscopy (PALM) and stochastic optical resolution microscopy (STORM)], the recruitment of fluorescently labelled host proteins to the adhesion site. Finally, we benefited from AFM to perform force adhesion spectroscopy measurements.

It is thought that the host cell membrane's cholesterol-rich lipid raft microdomains are instrumental in orchestrating the cell signalling response that leads to bacteria entry [Enninga and Rosenshine, 2009]. Previous research demonstrated that removing cholesterol from the cell plasma membrane can affect the ability of *Y. pseudotuberculosis* to enter macrophages (when bacteria were grown at 28°C, thus preventing the expression of the type III secretion system (T3SS) [Sato *et al.*, 2006]). In the present work, we extended this biochemical data by observing the recruitment of glycosylphosphatidylinositol (GPI)-anchored proteins that are known to be associated with lipid rafts. A GPI-anchor fused with the green fluorescent protein (GFP) was transiently expressed in HeLa cells. *Y. pseudotuberculosis* was adsorbed on a tipless AFM cantilever and labelled with 4',6'-diamidino-2-phenylindole (DAPI) for tracking purposes. Upon *Yersinia* contact with the host cell surface, the timescale of recruitment of the GPI-

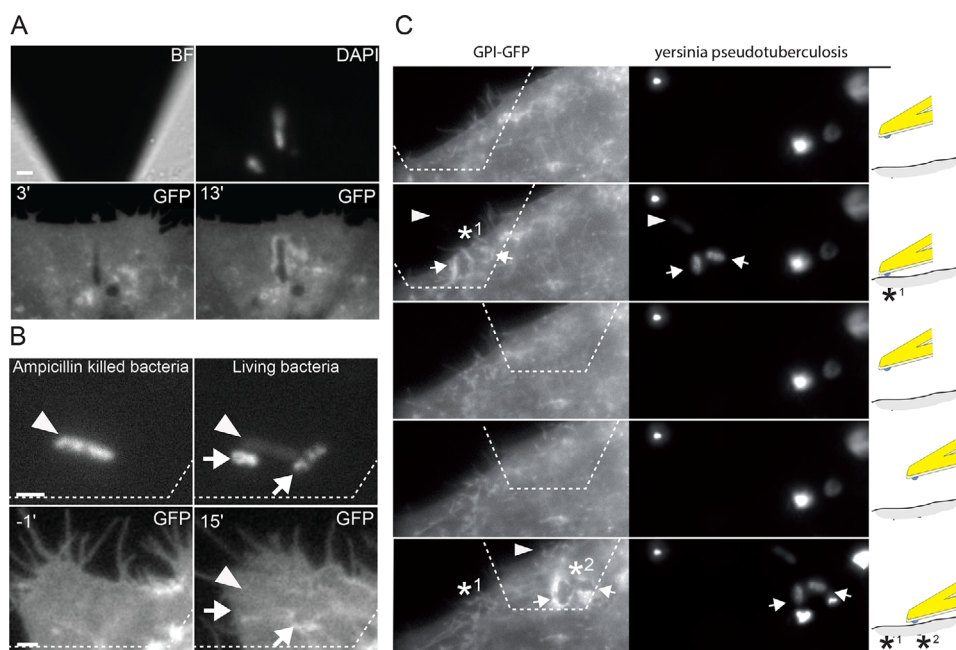
GFP chimera was monitored (Figure 1A and Supplementary Figure S1 and Movie S1). Landing the bacterium on the cell surface with a weak force (1–3 nN), we monitored the cellular distribution of the GPI-GFP molecules once the bacterium was brought into contact with the cell surface. The GPI-GFP recruitment showed a pattern starting at foci and resulted in the bacterium being surrounded by GPI-GFP constructs (Supplementary Figure S1). Furthermore, we observed specific routing of the construct around the bacteria (Figure 1A and Supplementary Movie S1). Importantly, using a fluorescent metabolic readout, we previously reported that *Y. pseudotuberculosis* once coated on the cantilever remains alive [Rodriguez-Emmenegger *et al.*, 2015].

In order to confirm that the recruitment was specific for live bacteria, we compared the respective capacities of live and dead *Yersiniae* to induce GPI-GFP clustering at the bacterium/cell surface interface. To this end, two sets of live bacteria were prepared. One set consisted of live bacteria that were coated onto the cantilever and then killed upon ampicillin treatment (arrowhead, Figure 1B). These bacteria were compared to live bacteria (arrows). In addition, live and dead bacteria were absorbed on the same cantilever to compare, at the same time, on the same cell, their influence on the cell signalling response (Figure 1B). A typical example is provided in Figure 1B; the lower panel (GFP channel inserts) shows GPI-GFP fluorescence at 1 min before and 15 min after contact. The ampicillin-killed bacteria were unable to recruit GPI-GFP proteins, most probably due the effect of this  $\beta$ -lactam on the cell wall. At the opposite, the recruitment was observed around the live bacteria (arrows Figure 1B and Supplementary Movie S2).

To assess the method's robustness after the initial host-pathogen interaction, we performed iterative measurements by retracting the bacterium-coated tip and moving it to other locations on the same cell (Figure 1C). We observed that the bacterium was stably adsorbed on the cantilever. This enabled us to monitor several GPI-GFP recruitment events with the same bacterium at different locations, on the same cell (Figure 1C). The patterns of recruitment were the same for the first contact and the subsequent ones. Hence, we demonstrate that GPI domains can be iteratively mobilised on the same cell surface by *Y. pseudotuberculosis* and that it requires living microorganisms.

**Figure 1 | GPI–GFP recruitment around bacteria**

(A) *Y. pseudotuberculosis* (grown at 28°C) were adsorbed on a tipless cantilever and brought into contact with a single HeLa cell transiently expressing the GPI–GFP construct. The top left panel show the shape of the tipless cantilever (observed in bright field (BF) mode) and DAPI-stained bacteria adsorbed on the cantilever. The time sequence of GPI–GFP recruitment around the bacteria is shown, with the time point (in minutes) indicated in the top left-hand corner. See Supplementary Movie S1. (B) Ampicillin-killed bacteria (arrowhead) and live bacteria (arrows) were adsorbed on the same tipless cantilever (upper panels). Note that the dead bacteria were partially bleached upon illumination (prior to adsorption of live bacteria). The time course of GPI–GFP recruitment around bacteria starts 1 min before cantilever engagement (–1') (see the time point in the top right-hand corner, bottom panels). At 15 min of contact, recruitment occurs around the live bacteria only (arrows). See Supplementary movie 2. Scale bars: 1 μm. (C) Panels show a HeLa cell expressing the GPI–GFP construct (first column) and DAPI-stained *Y. pseudotuberculosis* adsorbed on a tipless cantilever into contact (or not) with the cell surface (second column). When bacteria are in contact with the plasma membrane, we observe the GPI–GFP recruitment around the bacteria. The contact area is shown by an asterisk. The time interval between retraction and re-engagement was about 3 min. Only bacteria in contact with the cell are able to induce GPI–GFP clustering (arrows vs. arrowhead). Column 3 shows the position of the cantilever during the time. Dotted lines show the cantilever edges (B and C). Scale bars: 1 μm.



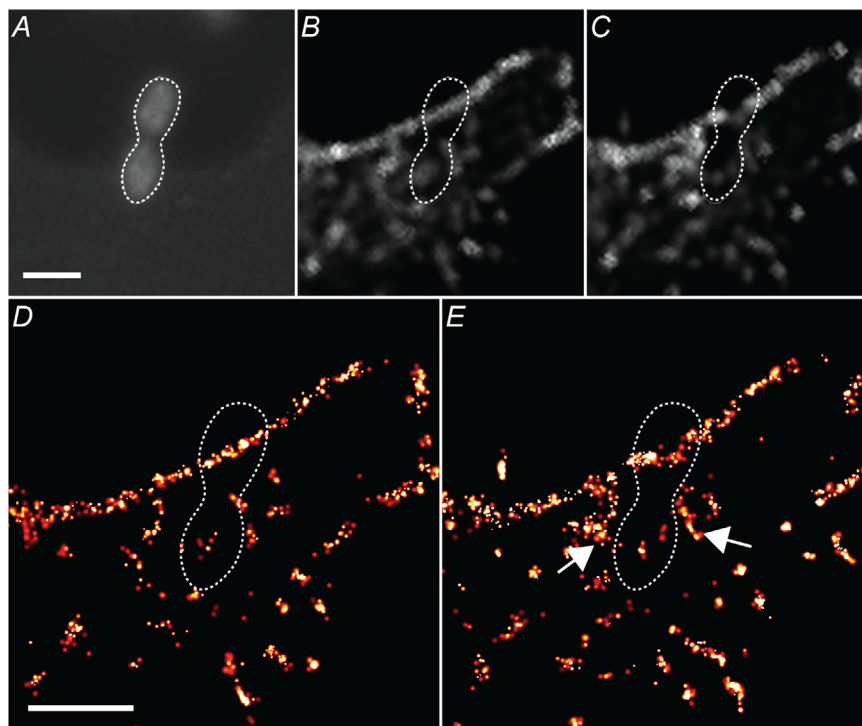
**Actin remodelling at the nanometre scale upon bacteria adhesion**

*Y. pseudotuberculosis* can be internalised via a zipper mechanism characterised by the tight apposition of invading bacteria with plasma membrane, enriched with actin filaments. We used PALM to examine with very high precision actin behaviour during AFM-driven bacterium–cell contact. To this end, we transiently expressed in HeLa cells an actin protein fused to the tandem dimer Eos photoactivable protein (tdEos-Actin) and performed similar experiments to those described above. We imaged in flat

area of the cell to easily visualise actin recruitment around the bacterium (Figure 2). The actin distribution was reminiscent of the early stage of an acting cup. Importantly, the actin recruitment was not observed when a cantilever with a spherical colloidal borosilicate glass probe was used (*i.e.*, actin accumulation was not observed with an inert substratum unless applying a high 15 nN force; Supplementary Figure S2). Hence, we show herein how to combine PALM fluorescence super-resolution technique with CLAM to accurately appreciate cell responses upon landed living microorganisms.

**Figure 2 | Actin polymerisation following bacterium-cell surface interaction**

Super-resolution PALM imaging of actin polymerisation around bacteria in contact with the surface of a HeLa cell expressing tdEos-actin. **(A)** *Y. pseudotuberculosis* adsorbed on the AFM cantilever. Actin was observed before **(B and D)** and 10 min after the bacteria have contacted the cell surface **(C and E)**. **(B)** and **(C)** Sum wild field image (SWF). **(D and E)** PALM image reconstruction. A localisation precision between 15 and 25 nm was used. SWF and PALM images were reconstructed in Zen 2011 SP3 software (ZEISS®).

**Bacteria-mediated post-translational modifications at the cell surface**

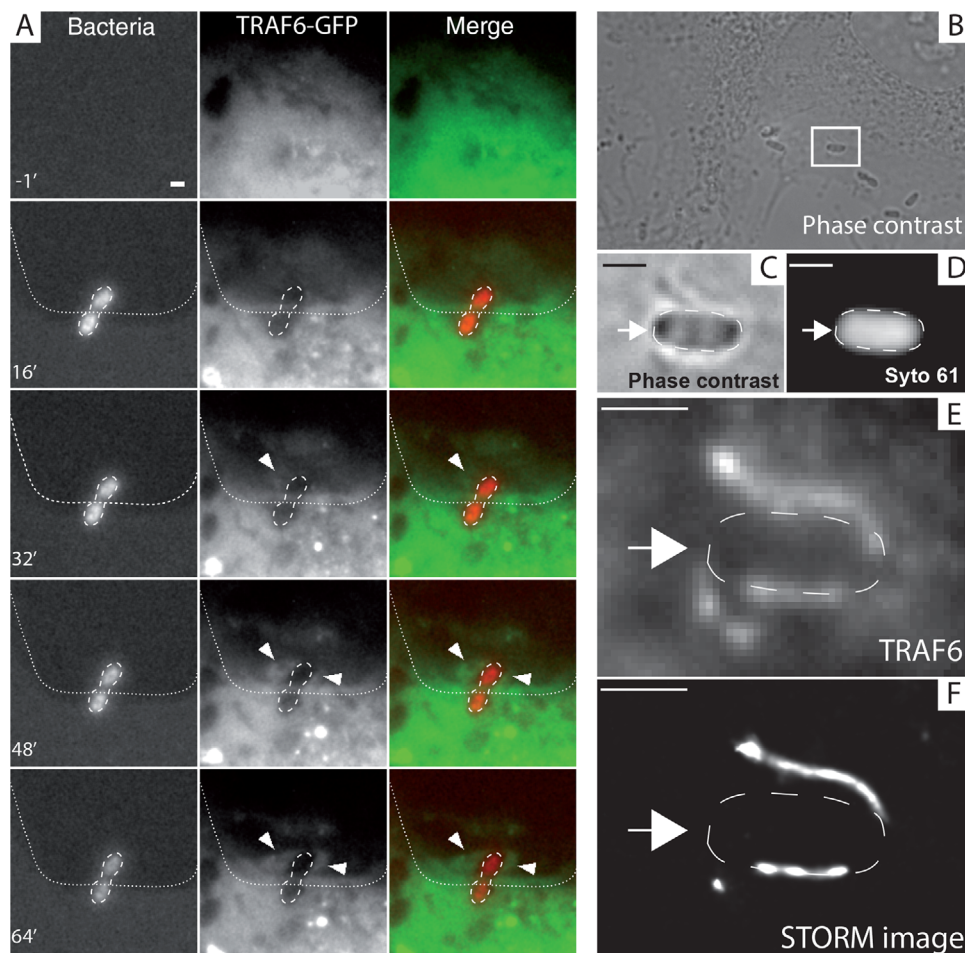
We next assessed the possibility to follow the recruitment of cytosolic molecules to the plasma membrane adhesion site of *Yersinia*. We targeted the small GTPase Tumour necrosis factor Receptor-Associated Factor 6 (TRAF6) as (i) it is well described to cycle between the cytosol and the membrane [Takaesu *et al.*, 2000], (ii) TRAF6 undergoes deubiquitination upon bacteria invasion although the mechanism is still debated [Perrett *et al.*, 2011], (iii) it belongs to the Toll-like receptors pathway [Kawai and Akira, 2007, 2010], which plays a central role in host cell recognition and response to microbial pathogens including for *Yersinia* [Faure *et al.*, 2000; Zhang and Bliska, 2003]. We used a cantilever functionalised with *Y. pseudotuberculosis* and monitored the interaction between the bacterium and the host cell transiently

expressing fluorescent-tagged TRAF6 (TRAF6-GFP; Figure 3A). TRAF6 can be observed using STORM imaging associated to *Yersinia*-containing vacuoles at early stages of infection (Figures 3B–3E). A clear recruitment was observed upon contact (Figure 3 and Supplementary Movie S3). This result confirms and extends previous reports, as we and others have shown that upon infection TRAF6 can be recruited to bacteria-containing vacuolar membranes [Walsh *et al.*, 2008; Dupont *et al.*, 2009]. Remarkably, to date, we thus achieved monitoring online TRAF6 at the cell surface during pathogen adhesion.

We then asked whether we could exploit our approach to learn more about host-pathogen interactions and obtain new insights on post-translational modifications of signalling molecules occurring during the adhesion step. This topic has been

**Figure 3 | TRAF6 proteins are recruited at the *Y. pseudotuberculosis* binding site**

(A) HeLa cells were transiently transfected to express a TRAF6-GFP construct. After adsorption on a cantilever, *Y. pseudotuberculosis* grown at 28°C interacted upon engagement with the cell surface. TRAF6 proteins recruitment was observed during interaction time started from 32 min (middle and left column). Bacteria were labelled with DAPI to be localised. See Supplementary Movie S3. (B–F) HeLa cell were transiently transfected to express a TRAF6-flag construct. After 40 min of infection with *Y. pseudotuberculosis*, cells were fixed then TRAF6 proteins were localised in TIRF (E) or STORM (F). Bacteria were labelled with SYTO® 60 red (D) Differential interference contrast image of the Hela cell infected by *Y. pseudotuberculosis* (B and C). (C–F) Zoom of the white rectangle of (B). Cantilever and bacterium were delimited respectively with dotted and dash line. Scale bar: 1 μm. For STORM image, bacteria were fixed with formalin (SIGMA®) and labelled with SYTO® 60 Red (Molecular Probe®: excitation/emission 652/678 nm). Flag epitope were revealed with Flag-M2 antibody (SIGMA®) and a secondary antibody labelled with an alexa 488 fluorophore. During acquisition, oxydative medium (50 mM MEA) was used. Before STORM acquisition, bacteria were imaged until SYTO® 60 fluorescence was bleach. Acquisition was performed on an ELYRA P1 microscope (ZEISS®). Image was processed using Zen 2011 SP3 software (ZEISS®). version: 8.1.6.484). For STORM image reconstruction, a localisation precision between 10 and 40 nm and a minimum photon count of 200 were used.

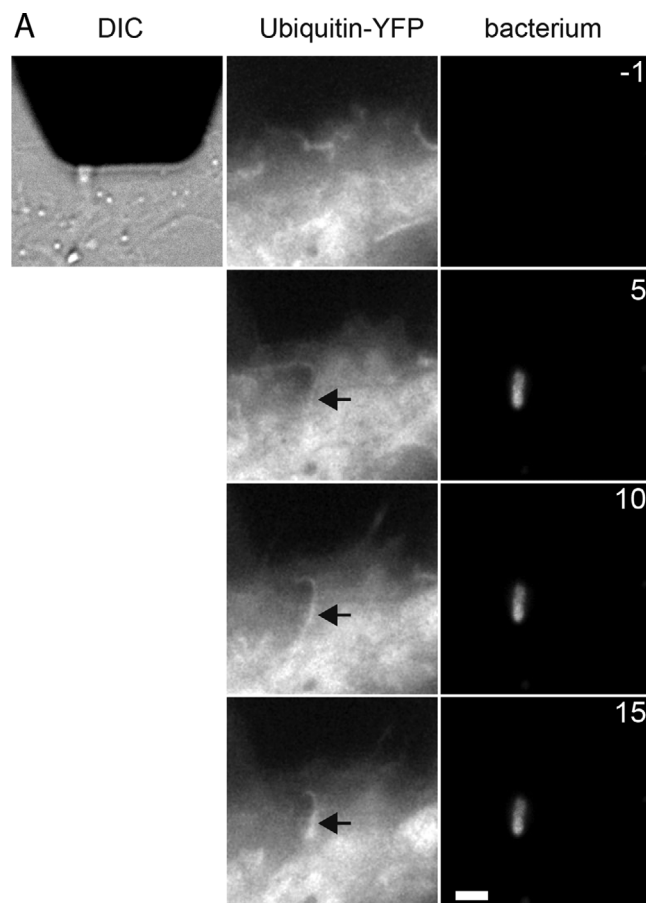


reinvestigated [Ribet and Cossart, 2010a] though, again, discriminating between adhesion and entry could not be examined with the accuracy developed now by our approach. We recorded the distribution

of transiently expressed yellow fluorescent-tagged ubiquitin (Ubi-YFP) during the interaction of the bacterium with the host cell surface (Figure 4 and Supplementary Movies S4 and S5).

**Figure 4 | Ubiquitylated-YFP is recruited at the *Y. pseudotuberculosis* binding site**

After adsorption on a cantilever, *Y. pseudotuberculosis* grown at 28°C was placed in contact with the cell surface (DIC, first column). HeLa cells transiently expressed a YFP-ubiquitin construct (second column). The bacterium was labelled with DAPI (third column). The recruitment of ubiquitylated-YFP was observed during the interaction (black arrows). Scale bar: 1  $\mu\text{m}$ . Time points in minutes are given in the upper right-hand corner of each picture of the second column. See Supplementary Movies S4 and S5.

**Bacterium–host cell adhesion forces**

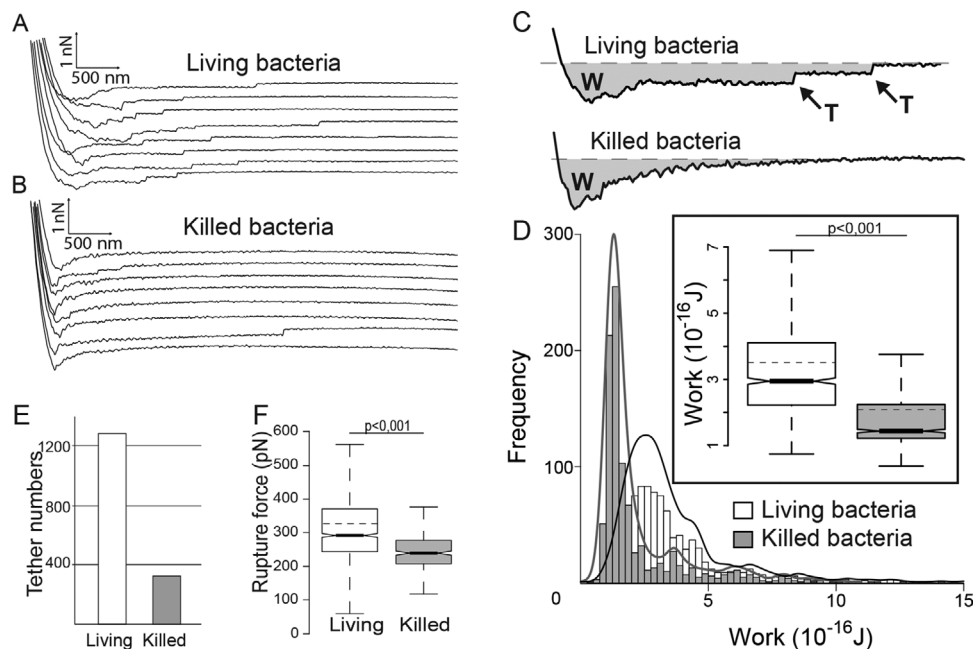
Importantly, while using the fluorescence-based approach described above, we were also able to exploit the AFM to perform force spectroscopy analysis. This allowed to carry out quantitative force measurements using cantilevers coated with living or dead bacteria. Thus, we could establish a correlation between the recruitment of the fluorescent-tagged molecules expressed in the host cell to the bacterial adhesion site and, the adhesion force capacity of the bacterium. First, bacteria were grown at 37°C in the presence of sodium oxalate and magnesium chloride (to allow expression of the T3SS and YadA adhesin). Then, bac-

teria bound to the cantilever were used either alive or killed upon glutaraldehyde treatment. We compared the adhesion of live and glutaraldehyde-killed bacterium (Figures 5A and 5B) and the work needed for detachment of either microorganism from the host cell surface [Puech *et al.*, 2005] (Figures 5C and 5D). There was a clear difference between live and killed bacteria (Figure 5D). Remarkably, the work values were similar to those reported by Puech *et al.* (2005). We also analysed the number of lipid tethers pulled from the cell membrane upon retraction of the bacterium bound to the cantilever (Figures 5C and 5E), and the related rupture forces (Figure 5F) [Müller



**Figure 5 | Interaction forces between the bacterium adsorbed on the cantilever and the host cell**

(A) Examples of force retraction curves obtained with live bacteria. (B) Examples of force retraction curves obtained with glutaraldehyde-killed bacteria. (C) The work corresponds to the grey area, calculated according to Puech et al. (2005). (D) Histogram and box plot (inset) of the frequency distribution of the work. (E) Total number of tethers (T, as indicated in the panel C) detected on the same number of retraction curves (1,024) for live and for dead bacteria. (F) Box plot of tether rupture forces for live and for killed bacteria. (E, F and D) Data correspond to three independent experiments giving a total number of 1,024 curves per condition. Notched boxplots are showing 1st quartile, median (line), mean (dashed), 3rd quartile. Whiskers extends to 1% and 99% of the data.



*et al.*, 2009; Mostowy *et al.*, 2011]. Adhesion, tether pulling and event rupture forces were all significantly increased for live bacteria (Figures 5E and 5F).

## Discussion

The multiparametric approach described in this work offers new opportunities. We first describe a method using AFM to nanoguide microorganisms. This permits to land bacteria on cells in which functional exploration of the recruitment dynamics of signalling molecules can be obtained. This analysis can be achieved at very high localisation precision (50 nm in this study). Moreover, this approach exploits the force spectroscopy capacity of AFM to conduct correlative studies. We validated the possibility to block physically the entry of *Y. pseudotuberculosis* at the adhesion step allowing to record the recruitment of host cell molecules expressed with a fluorescent tag

(uncoupling thus adhesion at the cell surface and internalisation of the bacterium). We could illustrate the recruitment of membrane proteins and unveil their dynamics upon iterative engagements. Moreover, we demonstrate the feasibility of monitoring a subset of post-translationally modified proteins. On the other hand, we could follow at the super-resolution level, a cell response mechanism by which the cell senses the adhesion of the bacterium by modulation of the actin subcortical network at the cell/substratum interface.

Currently, the bacterium adsorption on the cantilever step proved to be dependent on optimal growth condition (fresh preparation at the mid-exponential phase). Hopefully, we can envision two strategies for further development and ease of use. Chemical probes could covalently bind on the one hand the cantilever and, on the other hand, the bacterium targeting-specific binding sites. Alternatively,

one can use mechanical tethering devices based on differential pressure to fix bacteria to an apertured cantilever.

Importantly, for the infection field, the approach described herein will allow to tackle questions that so far remained unsolved concerning (i) a comprehensive analysis of the polarity of host protein recruitments following bacterial adhesion and (ii) the specific relationship between specific adhesins expressed on the bacterium and the recruitment of host signalling protein subsets. Methods to examine the secretion of bacterial effectors have already been described, such as (i)  $\beta$ -lactamase-based protein translocation assay monitoring the loss of Förster resonance energy transfer on sensor molecules expressed inside the host [Enninga and Rosenshine, 2009], (ii) mutagenised effectors capable of binding a fluorescent reagent once inside the host cell [Enninga *et al.*, 2005; Van Engelenburg and Palmer, 2008] and (iii) effector fusion with the complementary part of a split-GFP molecule expressed inside the host cell [Van Engelenburg and Palmer, 2010]. However, our approach makes it possible to challenge still untouched issues related to secretion systems. For instance, it will be feasible to monitor, at the cell level, the time required for new synthesis of effectors enough to induce a cell response. This approach also allows to accurately register the polarity of secretion and the distribution of either effectors and/or host cell signalling molecules. Using the same host cell/bacterium pair, it is also possible to compare bacterium-induced signalling responses before and after effector secretion. This breakthrough approach will thus open new possibilities to better investigate the action of bacterial effectors.

In terms of cellular interactions, by combining real-time force spectroscopy and (super-resolution) biophotonic measurements, the approach described in this work facilitates multiparametric correlated analysis of cell-to-cell interactions. Moreover, one can envision imaging the cell response to chemically modified cantilever surfaces (*e.g.*, tipless, pyramid-shaped tip, bead-coated). We demonstrated its power unveiling important angles of *Yersinia*–host cell interactions opening new avenues to investigate underestimated aspects of pathogen virulence. We document for the first time the controlled analysis of post-translationally modified signalling molecules at the bacteria adhesion site. The same approach could conceivably be extended beyond the field of infection

to study cell–cell and ligand–cell interactions particularly in cancer, neurobiology, metabolic diseases, developmental biology and as far as mechanobiology is concerned to monitor, while applying different forces, the effect of these interactions on the recruitment of cellular signalling molecules. CLAM is getting more popularised within the scientific community and mechanobiology is emerging as a new field to offer biophysical parameters that can complement molecular markers to characterise cells and tissues. Hence, our approach and the first results regarding signalling responses to cell–cell interactions revealed in the present work, represent an important seminal work for basic and applied science.

## Methods

### Adsorption of bacteria on AFM cantilevers

A 1/100 dilution of overnight pre-cultured *Y. pseudotuberculosis* (IP32777 strain) was cultured for 3 h in Luria Broth at 28°C or 37°C, depending on the experiment. Next, 1 ml of the bacterial suspension was added to a glass bottom dish (WillCo-dish) with DAPI or SYTO<sup>®</sup> 60 for 15 min at 37°C. Bacteria were rinsed three times in minimum essential media (MEM) without phenol red indicator (GIBCO) and resuspended in 2 ml of MEM containing 50 mM HEPES. Tipless cantilevers (DNP-O, spring constant: 0.06 N/m; Bruker) were cleaned with plasma oxygen and functionalised with 1/3000 (3-aminopropyl)trimethoxysilane in toluene for 30 min. This method was found optimal for the tip coating with *Y. pseudotuberculosis* and specific chemistry should be determined for each microorganism (or alternative methods may be used see discussion). The cantilevers were then rinsed (three times in toluene and three times in ethanol and dried) and then placed in contact with bacteria adhered to glass. Bacteria were killed either by a 120 min exposure to ampicillin (100  $\mu$ g/ml) at 28°C or by incubation in a 4% glutaraldehyde solution with unreacted aldehydes being quenched upon incubation in 150 mM glycine buffer. To force activation of the type III secretion system, the 1/100 dilution of overnight pre-culture of *Y. pseudotuberculosis* was cultured for 3 h in 2 $\times$  Yeast extract and Tryptone medium (2 $\times$ YT) supplemented with sodium oxalate (20 mM) and magnesium chloride (20 mM) at 37°C, as previously described [Auerbuch *et al.*, 2009].

### Microscopy and image analysis equipment and settings

HeLa cells were maintained in MEM containing 50 mM HEPES at room temperature. All imaging experiments were performed on an inverted optical microscope (Axiovert 200M; Zeiss). Fluorescent proteins (GFPs and YFPs) were imaged using a HXP120 light source and Zeiss filter FS38HE. The fibre's output was collimated and focused onto the back focal plane of a numerical aperture oil immersion objective (Plan-Apochromat 100x/1.44; Zeiss). The filtered emission was then imaged with a camera (CoolSNAP-ES; Photometrics). The microscope was driven by MetaMorph software (Molecular Device) and data were analysed using ImageJ software (<http://rsb.info.nih.gov/ij/>).

To quantify the recruitment of GPI–GFP molecules around bacteria during landing at the cell surface, intensity–distance line profiles (width 10 pixels) were extracted from four different 8-bit images representing different time points and analysed with the Fiji (NIH) software.

PALM was performed on a prototype system (serial number: 2701000006; Zeiss) composed of an Axio Observer Z1 SR microscopy platform, a numerical aperture oil immersion objective (Plan-Apochromat 100x/1.46; Zeiss) and a back-thinned EMCCD camera (iXon 897; Andor). Each final image was composed of about 3000 images (100 ms frame rate). The centroids of molecules were calculated and mapped using Zen 2011 SP3 software ZEISS®, version: 8.1.6.484). For the reconstruction, a localisation precision cut off between 15 and 25 nm and a minimum photon count of 2000 were used

### Atomic force microscopy

All experiments were performed at least five times (meaning bacterial cultures, catching and adhesion on cells) at room temperature using a commercial AFM (BioScope2 and BioScope Catalyst; Bruker) combined with an inverted optical microscope (Axiovert 200m; Zeiss). We used Bruker tipless AFM cantilevers with a nominal spring constant of 0.06 N/m. The spring constant was calibrated, using the thermal noise analysis in NanoScope Analysis software (version 7.30; Bruker). For adhesion experiments, the AFM was operated in force volume mode, in which the AFM records the deflection of the cantilever during vertical downward movement (extension) and upward movement (retraction) of the piezo scanner. The maximum retraction height of the cantilever was set to 10  $\mu\text{m}$  above the cell. Tip velocity was set to 20  $\mu\text{m/s}$ . The contact force was set to 3 nN during 100 ms with similar hydrodynamic drag exerted on tip coated with dead or live bacteria as experiments were performed in the same culture medium. Data analysis was done using in-house developed pyAF (python atomic force) software, version 1.5.0 [Popoff *et al.*, 2014]. This software was also used to analyse tethers, as previously described [Mostowy *et al.*, 2011]. The software scanned each retraction curve and computed the shape and size of binding-unbinding events by using a fuzzy logic algorithm [Kasas *et al.*, 2000]. Statistical significance was evaluated in a Student's *t*-test implemented in R software (version 2.10.0, <http://www.r-project.org>). The baseline was corrected as previously described [Friedrichs *et al.*, 2010], and the work was calculated according to Puech *et al.*'s method [Puech *et al.*, 2005]. First, a linear part of each curve was manually selected. Next, the area was calculated using Simpson's rule implemented in pyAF. A total of 1024 curves were analysed per condition.

For the non-coated cantilever experiment, we used a silicon nitride scanning microscopy probe with a colloidal 20  $\mu\text{m}$  borosilicate glass tip (CP-PNPL-BSG-C from sQube; spring constant: 0.08 N/m). A range of forces was applied (from 3 to 40 nN) by using the closed-loop scanner. The host cell–bacterium contact time was 15 min at least and 5000 PALM images were then acquired over 2 min using Zen software (ZEISS®) with a localisation precision of 50 nm.

### Author contribution

Y.C. carried out video-AFM, AFM-TIRF and AFM-PALM experiments, acquired and analysed the data

and wrote the manuscript. E.W. assisted the SR experiments performed fluorescence quantification. S.J. and M.P. carried out AFM experiments with bead-coated cantilevers and analysed the adhesion data. F.L. oversaw the experiments, analysed the data and wrote the manuscript.

### Acknowledgements

We thank A. Bongiovanni from the BICeL Facility for access to systems and technical advice. We would like to thank J. Warein for expert technical assistance, P.-H. Puech for valuable discussions and T. Melin, P.-E. Milhiet and G. Tran Van Nhieu for critical reading of the manuscript.

### Funding

This study was supported by funds from Univ. Lille 1 to M.P. and ANR (09-MIEN-020-01, 10-EQPX-04-01, 16), FEDER (12,001,407) to F.L.

### Conflict of interest statement

The authors have declared no conflict of interest.

### References

- Achtman, M., Zurth, K., Morelli, G., Torrea, G., Guiyoule, A. and Carniel, E. (1999). *Yersinia pestis*, the cause of plague, is a recently emerged clone of *Yersinia pseudotuberculosis*. *Proc. Natl. Acad. Sci. U.S.A.* **96**, 14043–14048
- Alsteens, D., Beaussart, A., El-Kirat-Chatel, S., Sullan, R. M. A. and Dufrène, Y. F. (2013). Atomic force microscopy: A new look at pathogens. *PLoS Pathog.* **9**, e1003516
- Auerbuch, V., Golenbock, D. T. and Isberg, R. R. (2009). Innate immune recognition of *Yersinia pseudotuberculosis* type III secretion. *PLoS Pathog.* **5**, e1000686
- Cantey, J. R., Lushbaugh, W. B. and Inman, L. R. (1981). Attachment of bacteria to intestinal epithelial cells in diarrhea caused by *Escherichia coli* strain RDEC-1 in the rabbit: stages and role of capsule. *J. Infect. Dis.* **143**, 219–230
- Chung, L. K. and Bliska, J. B. (2015). *Yersinia* versus host immunity: how a pathogen evades or triggers a protective response. *Curr. Opin. Microbiol.* **29**, 56–62
- Cossart, P. and Sansonetti, P. J. (2004). Bacterial invasion: the paradigms of enteroinvasive pathogens. *Science* **304**, 242–248
- Dewoody, R. S., Merritt, P. M. and Marketon, M. M. (2013). Regulation of the *Yersinia* type III secretion system: traffic control. *Front. Cell. Infect. Microbiol.* **3**, 4
- Dupont, N., Lacas-Gervais, S., Bertout, J., Paz, I., Freche, B., Van Nhieu, G. T., van der Goot, F. G., Sansonetti, P. J. and Lafont, F. (2009). *Shigella* phagocytic vacuolar membrane remnants participate in the cellular response to pathogen invasion and are regulated by autophagy. *Cell Host Microbe* **6**, 137–149
- Dupont, N., Temime-Smaali, N. and Lafont, F. (2010). How ubiquitination and autophagy participate in the regulation of the cell response to bacterial infection. *Biol. Cell* **102**, 621–634

- Van Engelenburg, S. B. and Palmer, A. E. (2008). Quantification of real-time Salmonella effector type III secretion kinetics reveals differential secretion rates for SopE2 and SptP. *Chem. Biol.* **15**, 619–628
- Van Engelenburg, S. B. and Palmer, A. E. (2010). Imaging type-III secretion reveals dynamics and spatial segregation of Salmonella effectors. *Nat. Methods* **7**, 325–330
- Enninga, J., Mounier, J., Sansonetti, P. and Tran Van Nhieu, G. (2005). Secretion of type III effectors into host cells in real time. *Nat. Methods* **2**, 959–965
- Enninga, J. and Rosenshine, I. (2009). Imaging the assembly, structure and activity of type III secretion systems. *Cell. Microbiol.* **11**, 1462–1470
- Faure, E., Equils, O., Sieling, P. A., Thomas, L., Zhang, F. X., Kirschning, C. J., Polentarutti, N., Muzio, M. and Arditi, M. (2000). Bacterial lipopolysaccharide activates NF-kappaB through toll-like receptor 4 (TLR-4) in cultured human dermal endothelial cells. Differential expression of TLR-4 and TLR-2 in endothelial cells. *J. Biol. Chem.* **275**, 11058–11063
- Feuillie, C., Vitry, P., McAleer, M. A., Kezic, S., Irvine, A. D., Geoghegan, J. A. and Dufrene, Y. F. (2018). Adhesion of *Staphylococcus aureus* to corneocytes from atopic dermatitis patients is controlled by natural moisturizing factor levels. *MBio* **9**
- Friedrichs, J., Helenius, J. and Muller, D. J. (2010). Quantifying cellular adhesion to extracellular matrix components by single-cell force spectroscopy. *Nat. Protoc.* **5**, 1353–1361
- Harke, B., Chacko, J. V., Haschke, H., Canale, C. and Diaspro, A. (2012). A novel nanoscopic tool by combining AFM with STED microscopy. *Opt. Nanoscopy* **1**, 3
- Hoffmann, I., Eugene, E., Nassif, X., Couraud, P. O. and Bourdoulous, S. (2001). Activation of ErbB2 receptor tyrosine kinase supports invasion of endothelial cells by *Neisseria meningitidis*. *J. Cell Biol.* **155**, 133–143
- Janel, S., Werkmeister, E., Bongiovanni, A., Lafont, F. and Barois, N. (2017). CLAFEM: Correlative light atomic force electron microscopy. *Methods Cell Biol.* **140**, 165–185
- Kasas, S., Riederer, B. M., Catsicas, S., Cappella, B. and Dietler, G. (2000). Fuzzy logic algorithm to extract specific interaction forces from atomic force microscopy data. *Rev. Sci. Instrum.* **71**, 2082–2086
- Kawai, T. and Akira, S. (2007). TLR signaling. *Semin. Immunol.* **19**, 24–32
- Kawai, T. and Akira, S. (2010). The role of pattern-recognition receptors in innate immunity: update on Toll-like receptors. *Nat. Immunol.* **11**, 373–384
- Kawai, T. and Akira, S. (2011). Toll-like receptors and their crosstalk with other innate receptors in infection and immunity. *Immunity* **34**, 637–650
- McCall-Culbreath, K. D., Li, Z. and Zutter, M. M. (2008). Crosstalk between the alpha2beta1 integrin and c-met/HGF-R regulates innate immunity. *Blood* **111**, 3562–3570
- Mikula, K. M., Kolodziejczyk, R. and Goldman, A. (2013). Yersinia infection tools—Characterization of structure and function of adhesins. *Front. Cell. Infect. Microbiol.* **2**, 169
- Mostowy, S., Janel, S., Forestier, C., Roduit, C., Kasas, S., Pizarro-Cerdá, J., Cossart, P. and Lafont, F. (2011). A role for septins in the interaction between the *Listeria monocytogenes* INVASION PROTEIN InIB and the Met receptor. *Biophys. J.* **100**, 1949–1959
- Müller, D. J., Helenius, J., Alsteens, D. and Dufrene, Y. F. (2009). Force probing surfaces of living cells to molecular resolution. *Nat. Chem. Biol.* **5**, 383–390
- Perrett, C. A., Lin, D. Y.-W. and Zhou, D. (2011). Interactions of bacterial proteins with host eukaryotic ubiquitin pathways. *Front. Microbiol.* **2**, 143
- Popoff, M., Janel, S., Bovio, S., Dupres, V., Ciczora, Y. and Lafont, F. (2014). *An Atomic Force Curve Analysis Software*. In: EuroPython, Berlin
- Prystopiuk, V., Feuillie, C., Herman-Bausier, P., Viela, F., Alsteens, D., Pietrocola, G., Speziale, P. and Dufrene, Y. F. (2018). Mechanical forces guiding *Staphylococcus aureus* cellular invasion. *ACS Nano* **12**, 3609–3622
- Puech, P. H., Taubenberger, A., Ulrich, F., Krieg, M., Muller, D. J. and Heisenberg, C. P. (2005). Measuring cell adhesion forces of primary gastrulating cells from zebrafish using atomic force microscopy. *J. Cell Sci.* **118**, 4199–4206
- Ribet, D. and Cossart, P. (2010a). Pathogen-mediated posttranslational modifications: A re-emerging field. *Cell* **143**, 694–702
- Ribet, D. and Cossart, P. (2010b). Post-translational modifications in host cells during bacterial infection. *FEBS Lett.* **584**, 2748–2758
- Rodriguez-Emmenegger, C., Janel, S., de los Santos Pereira, A., Bruns, M. and Lafont, F. (2015). Quantifying bacterial adhesion on antifouling polymer brushes via single-cell force spectroscopy. *Polym. Chem.* **31**
- Sato, Y., Kaneko, K., Sasahara, T. and Inoue, M. (2006). Novel pathogenetic mechanism in a clinical isolate of *Yersinia enterocolitica* KU14. *J. Microbiol.* **44**, 98–105
- Suzuki, T., Franchi, L., Toma, C., Ashida, H., Ogawa, M., Yoshikawa, Y., Mimuro, H., Inohara, N., Sasakawa, C. and Nunez, G. (2007). Differential regulation of caspase-1 activation, pyroptosis, and autophagy via Ipaf and ASC in *Shigella*-infected macrophages. *PLoS Pathog.* **3**, e111
- Takaesu, G., Kishida, S., Hiyama, A., Yamaguchi, K., Shibuya, H., Irie, K., Ninomiya-Tsuji, J. and Matsumoto, K. (2000). TAB2, a novel adaptor protein, mediates activation of TAK1 MAPKKK by linking TAK1 to TRAF6 in the IL-1 signal transduction pathway. *Mol. Cell* **5**, 649–658
- Travassos, L. H., Carneiro, L. A., Ramjeet, M., Hussey, S., Kim, Y. G., Magalhães, J. G., Yuan, L., Soares, F., Chea, E., Le Bourhis, L., Boneca, I. G., Allaoui, A., Jones, N. L., Nuñez, G., Girardin, S. E. and Philpott, D. J. (2010). Nod1 and Nod2 direct autophagy by recruiting ATG16L1 to the plasma membrane at the site of bacterial entry. *Nat. Immunol.* **11**, 55–62
- Walsh, M. C., Kim, G. K., Maurizio, P. L., Molnar, E. E. and Choi, Y. (2008). TRAF6 autoubiquitination-independent activation of the NFkappaB and MAPK pathways in response to IL-1 and RANKL. *PLoS One* **3**, e4064
- Xiao, J. and Dufrene, Y. F. (2016). Optical and force nanoscopy in microbiology. *Nat. Microbiol.* **1**, 16186
- Zhang, Y. and Bliska, J. B. (2003). Role of Toll-like receptor signaling in the apoptotic response of macrophages to *Yersinia* infection. *Infect. Immun.* **71**, 1513–1519

Received: 19 October 2018; Revised: 5 December 2018; Accepted: 6 December 2018; Accepted article online: 24 January 2019